

Article

# An Electrochemical Sensor for Trimethoprim Based on a Magnetic Molecularly Imprinted Carbon Paste Electrode

Peng Liu <sup>†</sup>, Ruiying Zhang <sup>†</sup>, Liyan Zheng <sup>\*</sup> and Qiue Cao <sup>\*</sup>

Key Laboratory of Medicinal Chemistry for Natural Resource, School of Chemical Science and Technology, Yunnan University, No. 2 North Cuihu Road, Kunming 650091, China; pliu@ynu.edu.cn (P.L.); zhangruiyingynu@163.com (R.Z.)

<sup>\*</sup> Correspondence: zhengliyan@ynu.edu.cn (L.Z.); qecao@ynu.edu.cn (Q.C.)

<sup>†</sup> These authors contributed equally to this work.

**Abstract:** In order to achieve simple, rapid, and highly sensitive detection of trimethoprim (TMP), a magnetic molecularly imprinted carbon paste electrode (MCPE) was prepared by drop-coating magnetic molecularly imprinted polymer (MIP@Fe<sub>3</sub>O<sub>4</sub>@MWNTs) on the surface of reduction graphene oxide (rGO)/MCPE doped with Fe<sub>3</sub>O<sub>4</sub>@MWNTs. The introduction of multi-walled carbon nanotubes (MWNTs) and rGO served as dual signal-amplification materials, which can improve the response sensitivity of the sensor. In addition, the magnetic interaction between the substrate electrode and the molecularly imprinted material was beneficial to increasing the stability of the sensor. As expected, the electrochemical sensor not only showed sensitivity and selectivity for the detection of TMP, but it also possessed good stability. The detection range for TMP was  $4.0 \times 10^{-9}$ – $5.0 \times 10^{-4}$  mol/L, and the detection limit was  $1.2 \times 10^{-9}$  mol/L. The response performance varied within 10% when the sensor was placed for more than 2 months and used more than 60 times. The spiked recoveries of TMP in environmental water samples, urine samples, and pharmaceuticals (drugs) were between 91% and 110%, and the relative standard deviation (RSD) was within 5%.

**Keywords:** trimethoprim; molecular imprinting technique; electrochemical sensor



**Citation:** Liu, P.; Zhang, R.; Zheng, L.; Cao, Q. An Electrochemical Sensor for Trimethoprim Based on a Magnetic Molecularly Imprinted Carbon Paste Electrode. *Chemosensors* **2023**, *11*, 339. <https://doi.org/10.3390/chemosensors11060339>

Academic Editor: Núria Serrano

Received: 16 May 2023

Revised: 3 June 2023

Accepted: 6 June 2023

Published: 8 June 2023



**Copyright:** © 2023 by the authors. Licensee MDPI, Basel, Switzerland. This article is an open access article distributed under the terms and conditions of the Creative Commons Attribution (CC BY) license (<https://creativecommons.org/licenses/by/4.0/>).

## 1. Introduction

Trimethoprim is a broad-spectrum antimicrobial agent that can be used to treat respiratory tract infections, digestive tract infections, typhoid, and meningitis. In addition, it can be used in combination with other drugs to increase their antibacterial effect. For example, in combination with sulfonamide, its efficacy can be increased dozens of times. Therefore, TMP is not only widely used in medical treatment but also as a veterinary antimicrobial potentiator in aquaculture [1], which leads to a substantial increase in the drug resistance of TMP. It was reported that the resistance rate of *E. coli* to TMP exceeded 70% [2]. In addition, TMP can also cause bone marrow micronucleus suppression and some other adverse effects, and excessive doses can cause kidney and liver damage [3]. Therefore, it is necessary to restrict the use of TMP in clinical settings, as well as in aquaculture. To safeguard human health from this specific risk, a maximum residue limit was established in China, the European Union, and other regulatory agencies for TMP of 100 ppb [4]. Consequently, sensitive, accurate, and rapid detection of TMP is important to control its abuse in daily life [5].

The most commonly used detection methods for TMP included liquid chromatography with a tunable absorbance detector [6], liquid chromatography tandem mass spectrometry [7,8], UV-visible spectroscopy [9], and capillary electrophoresis [10]. In addition, considering that TMP itself can be oxidized at a voltage near 1.1 V, there have been many reports on the determination of TMP via electrochemical analysis methods. Most of these electrochemical methods were based on glassy carbon electrodes modified with signal amplification materials, such as carbon nanomaterials and their composites. However, these

electrochemical sensors possessed low sensitivity or limited selectivity [11–20]. To improve the response selectivity of electrochemical sensors, molecularly imprinted materials are introduced as selective recognition elements to upgrade their performance. Molecularly imprinted material is a cross-linked polymer with a three-dimensional mesh structure (called an imprinted site) that matches the template in both spatial structure and functional groups; it is prepared by using the target as a template based on molecular imprinting technology [11]. Therefore, this material shows high recognition selectivity and structure-effect predetermination for the target, and it possesses good stability, strong environmental tolerance, and reusability [18].

Electrochemical sensors modified with molecularly imprinted materials are called molecularly imprinted electrochemical sensors. This kind of sensor combines the advantages of electrochemical sensors and molecularly imprinted materials, along with high sensitivity and good selectivity, which has gained wide attention in the analysis of trace components in complex systems. Research on TMP molecularly imprinted electrochemical sensors has been reported in a few literatures. For example, Silva et al. [21] and Wei et al. [22] prepared TMP molecularly imprinted sensors by modifying TMP molecularly imprinted polymers on graphene-modified glassy carbon electrodes and bare glassy carbon electrodes via electropolymerization and in-situ polymerization, respectively. However, the sensitivity of these two sensors was not ideal, and the detection limits were  $3.2 \times 10^{-8}$  mol/L and  $1.3 \times 10^{-7}$  mol/L, respectively. In addition, the current molecularly imprinted electrochemical sensors still meet the problems of easy peeling of the modified imprinted membrane, which limit the application in the determination of TMP.

In order to further improve the detection sensitivity and stability of the TMP molecularly imprinted electrochemical sensors, MWNTs and rGO were used as the dual signal-amplifying materials in this study.  $\text{Fe}_3\text{O}_4$ @MWNTs were applied not only as the carrier to prepare the magnetic molecularly imprinted polymers of TMP, but also as a magnetic component of MCPE. Then, MIP@ $\text{Fe}_3\text{O}_4$ @MWNTs were dropwise coated on the surface of rGO/MCPE to fabricate a TMP molecularly imprinted electrochemical sensor (MIP@ $\text{Fe}_3\text{O}_4$ @MWNTs/rGO/MCPE). The stability of the sensor was attributed to the magnetic interaction between the molecularly imprinted material and the substrate electrode. Thus, a highly sensitive electrochemical analysis method for the determination of TMP was established.

## 2. Materials and Methods

### 2.1. Reagents and Instruments

#### 2.1.1. Apparatus and Instruments

The cyclic voltammetry (CV) and differential pulse voltammetry (DPV) were carried out on a CHI 760E electrochemical workstation (Shanghai CH Instruments Co., Shanghai, China). Electrochemical impedance spectroscopy (EIS) was performed with Autolab302N (Metrohm, Utrecht, Netherlands). All of the electrochemical data were obtained from a three-electrode cell using a bare or modified carbon paste electrode (CPE, 2 mm diameter) as the working electrode, a saturated calomel electrode (SCE) as the reference electrode, and a platinum wire electrode as the counter electrode, respectively. Other instruments were used, including a Nova 450 scanning electron microscope (SEM, FEI, Hillsboro, OR, USA) and a thermostatic oscillator (Tai-cang Experimental Equipment Factory, Taicang, Jiangsu, China). A H1850 desktop high-speed centrifuge (Xiangyi Experimental Instrument Company, Changsha, Hunan, China). UV-vis spectra of solutions were measured using a UV-2700 UV-vis spectrophotometer (Shimadzu, Kyoto, Japan).

#### 2.1.2. Reagents and Chemicals

Trimethoprim (TMP,  $\geq 98\%$ ), sulfamethoxazole (SMZ,  $\geq 98\%$ ), sulfadiazin (SDZ,  $\geq 98\%$ ) and cephalixin (CAX,  $\geq 98\%$ ) were purchased from the Institute for Identification of Pharmaceutical and Biological Products (China). Glucose (Glu) was purchased from Xilong Chemical Industry. Urea (99%) is the product of Chinese medicine reagent. Methylalanine

acid (MAA) and 2-acetamide acrylic acid (AAA) were purchased from Sigma-Aldrich Corporation (St. Louis, MI, USA). Acrylamide (AM), N-allyl urea (NAU), and carboxylated multi-walled carbon nanotubes (MWNTs-COOH) were purchased from Aladdin Ltd. (Shanghai, China). Glycol dimethacrylate (EGDMA) and azodiisobutyronitrile (AIBN) were purchased from Shanghai Reagent Plant No. 4 (China). The former needs to be purified by vacuum distillation before use, and the latter by ethanol recrystallization before use. Potassium ferricyanide was purchased from Aladdin Ltd. (Shanghai, China). Graphite powder was purchased from Alfa Aesar Inc. (Shanghai, China). Other reagents used in the experiment were purchased from Sinopharm Chemical Reagent Co., Ltd. (Shanghai, China). Unless otherwise stated, all reagents used in the experiment were analytically pure or above, and the water was ultra-pure.

## 2.2. Preparation of $\text{Fe}_3\text{O}_4$ @MWNTs

$\text{Fe}_3\text{O}_4$ @MWNTs magnetic composites were prepared by the co-precipitation method, and the basic procedure was as follows [23]: 1.7 g of  $(\text{NH}_4)_2\text{Fe}(\text{SO}_4)_2 \cdot 6\text{H}_2\text{O}$  and 2.5 g of  $\text{NH}_4\text{Fe}(\text{SO}_4)_2 \cdot 12\text{H}_2\text{O}$  were added to a round-bottom flask containing 200 mL of water, and ultra-sonicated to disperse uniformly, followed by the addition of 2 g of carboxylated multi-walled carbon nanotubes, and then ultra-sonicated for about 10 min. Next, 10 mL of 8 mol/L ammonia were added dropwise to the above mixed solution, and the reaction was stirred at 50 °C (300 r/min) for 30 min under the condition of pH 11–12 to obtain a black suspension. The products were separated with a magnet, then washed with water and ethanol for 2–3 times, respectively, and then dried under vacuum to obtain  $\text{Fe}_3\text{O}_4$ @MWNTs.

## 2.3. Preparation of Magnetic Molecular Imprinted and Non-Imprinted Polymers of TMP

MIP@ $\text{Fe}_3\text{O}_4$ @MWNTs were prepared by the surface-imprinting method using  $\text{Fe}_3\text{O}_4$ @MWNTs as the carrier. The procedure was described as follows: 29 mg (0.1 mmol) of TMP (template molecule) and 51.6 mg (0.4 mmol) of AAA (functional monomer) were weighed and added into a round-bottom flask containing 20 mL of acetonitrile, and ultrasonicated for 30 min to fully combine TMP with AAA. Next, 0.1 g of  $\text{Fe}_3\text{O}_4$ @MWNTs and 30 mg of AIBN (initiator) were added, and then they were ultrasonicated for 10 min to make  $\text{Fe}_3\text{O}_4$ @MWNTs uniformly disperse and AIBN fully dissolve. Further, 1189.3 mg (6 mmol) of EGDMA (cross-linking agent) were added. The reaction tube was quickly sealed and reacted at 64 °C for 24 h. After that, the polymer was separated by centrifugation and extracted through Soxhlet extraction using methanol–acetic acid with a volume ratio of 8:2 as solvent to remove the template molecule TMP. Then, it was washed with methanol until neutral and dried under vacuum to obtain MIP@ $\text{Fe}_3\text{O}_4$ @MWNTs. The preparation of non-imprinted polymers (NIP@ $\text{Fe}_3\text{O}_4$ @MWNTs) was basically the same as that of MIP@ $\text{Fe}_3\text{O}_4$ @MWNTs, except that the template TMP was not added.

## 2.4. Preparation of TMP Molecularly Imprinted Electrodes

Preparation of MCPE: 10 mg of graphite powder and 10 mg of  $\text{Fe}_3\text{O}_4$ @MWNTs were weighed and mixed well in a round-bottom flask, 15  $\mu\text{L}$  of paraffin oil were added, and then ground and mixed to obtain a paste. The above paste was filled into a polytetrafluoroethylene tube ( $\varphi = 2$  mm), compacted, and inserted into a copper wire to lead it out from the other end. After standing at room temperature for 12 h, the electrode was polished until the surface was mirror-like. Meanwhile, a stable cyclic voltammogram in 5 mmol/L potassium ferricyanide solution could be obtained by the electrode.

Preparation of rGO/MCPE: 0.5 mg of graphene oxide were dispersed in 0.1 mol/L of  $\text{Na}_2\text{SO}_4$  solution (5.0 mL). Then, the obtained MCPE was placed in it as a working electrode, followed by electrodeposition at  $-1.4$  V for 500 s. Finally, the electrode was removed, rinsed well with water, and dried naturally at room temperature.

Preparation of MIP@ $\text{Fe}_3\text{O}_4$ @MWNTs/rGO/MCPE: Firstly, chitosan was ultrasonically dissolved in 0.05 mol/L acetic acid solution to obtain a chitosan solution with concentration of 0.5%. Then, 4 mg of MIP@ $\text{Fe}_3\text{O}_4$ @MWNTs were added to 1 mL of the above

chitosan solution and ultrasonicated for 30 min to make the MIP@Fe<sub>3</sub>O<sub>4</sub>@MWNTs fully disperse. Then, 7 µL of the above dispersion were dropwise coated on the surface of rGO/MCPE and dried under an infrared lamp. The preparation of the non-imprinted sensor (NIP@Fe<sub>3</sub>O<sub>4</sub>@MWNTs/rGO/MCPE) was the same as the above procedure, except that MIP@Fe<sub>3</sub>O<sub>4</sub>@MWNTs/rGO/MCPE was replaced by NIP @Fe<sub>3</sub>O<sub>4</sub>@MWNTs/rGO/MCPE. The prepared electrodes were stored in a 4 °C refrigerator for later use.

### 2.5. Equilibrium Adsorption Experiments of Imprinted and Non-Imprinted Polymers

First, 5 mg of the imprinted polymer MIP@Fe<sub>3</sub>O<sub>4</sub>@MWNTs or the non-imprinted polymer NIP@Fe<sub>3</sub>O<sub>4</sub>@MWNTs were added to 10 mL of TMP ethanol solution with a concentration of 20 µg/mL. The polymer was dispersed by ultrasonication for 5 min and then shaken at a constant temperature (25 °C) for 3 h at 160 r/min. Followed by magnetic separation, the concentration of TMP in the supernatant was measured at 287 nm in the UV–visible spectrum by a standard curve. The adsorption amount of TMP was equal to the difference between the total added amount and the amount in the supernatant. The equilibrium adsorption amount (Q) of the polymer was calculated as the amount of substrate adsorbed per unit mass of polymer (mg/g). The imprinting factor (IF) was used to evaluate the selectivity of each MIP against the template for which was synthesized in the presence of the other NIPs. The adsorption selectivity factor (IF value) was calculated as the ratio of the adsorption amount of imprinted polymer to that of non-imprinted polymer under the same condition; in brief,  $IF = Q_{MIP}/Q_{NIP}$ .

### 2.6. Electrochemical Testing Conditions

The prepared imprinted electrode, saturated calomel electrode, and platinum wire electrode constituted a three-electrode system. Cyclic voltammetry (CV), electrochemical impedance spectroscopy (EIS), and differential pulse voltammetry (DPV) were performed in a 10-mL electrolytic cell. The CV and EIS were performed in 0.1 mol/L KCl solution containing 5.0 mmol/L K<sub>3</sub>[Fe(CN)<sub>6</sub>], and the DPV was performed in 0.1 mol/L H<sub>2</sub>SO<sub>4</sub> solution containing 0.1 mol/L KCl. The sweep voltage range of CV was between −0.2 and 0.6 V with a sweep rate of 100 mV/s; the open circuit voltage, high frequency, low frequency, and amplitude selected for EIS analysis were 0.2 V,  $1.0 \times 10^5$  Hz, 0.03 Hz, and 0.01 V, respectively. DPV measurement required incubating the working electrode in an electrolyte solution containing TMP for 5 min, followed by a sweep between 0.7 and 1.4 V at a rate of 50 mV/s. To investigate the selectivity of the sensor, SMZ, SDZ, CAX, GLU, and urea with concentration at  $1.0 \times 10^{-5}$  mol/L are added in an electrolyte solution, respectively, incubated for 5 min, and followed by DPV measurement with a sweep between 0.7 and 1.4 V at a rate of 50 mV/s. To study the anti-interference ability of the sensor, the effects of different interfering substances on the peak current of MIP@Fe<sub>3</sub>O<sub>4</sub>@MWNTs/rGO/MCPE for  $1.0 \times 10^{-5}$  mol/L TMP were measured. For the regeneration of the sensor, after each measurement, the electrode needs to be ultrasonically cleaned with ethanol for ~3–5 min, and then rinsed with water before it is used again. Furthermore, the electrode was stored in pure water in a refrigerator at 4 °C.

### 2.7. Sample Preparation

Environmental water samples and human urine samples: Environmental water samples (Kunming Panlong River water samples) and healthy human urine were taken as real samples, centrifuged at 8000 r/min for 8 min, and the supernatant was taken for analysis.

Cefadroxil capsules: Take 10 commercially available capsules, remove the capsules, weigh 1/10th (equivalent to 12.5 mg TMP, i.e., the indicated amount of TMP in one capsule), dissolve with water, and fix the volume to 250 mL.

### 3. Results

#### 3.1. Characterization of Molecularly Imprinted Electrochemical Sensor

The morphologies of  $\text{Fe}_3\text{O}_4$ @MWNTs,  $\text{MIP@Fe}_3\text{O}_4$ @MWNTs, rGO/MCPE, and  $\text{MIP@Fe}_3\text{O}_4$ @MWNTs/rGO/MCPE were observed by a scanning electron microscope (SEM). As shown in Figure 1,  $\text{Fe}_3\text{O}_4$  nanoparticles were uniformly dispersed on the surface of the multi-walled carbon nanotubes. The magnetic molecularly imprinted polymer prepared with  $\text{Fe}_3\text{O}_4$ @MWNTs as a carrier prepared by surface-imprinting technology showed a uniform spherical structure, which was beneficial to ensure the reproducibility of the imprinted sensor. The reduced graphene oxide on the surface of the magnetic carbon paste electrode by the electroreduction method displayed a relatively flat structure, and distinct rGO sheets could be observed. The  $\text{MIP@Fe}_3\text{O}_4$ @MWNTs were modified by drop-coating on the rGO/MCPE surface with chitosan as a binder; this also formed a film. In addition, the film surface was complete and basically flat, and the imprinted polymer in the film was dispersed uniformly.

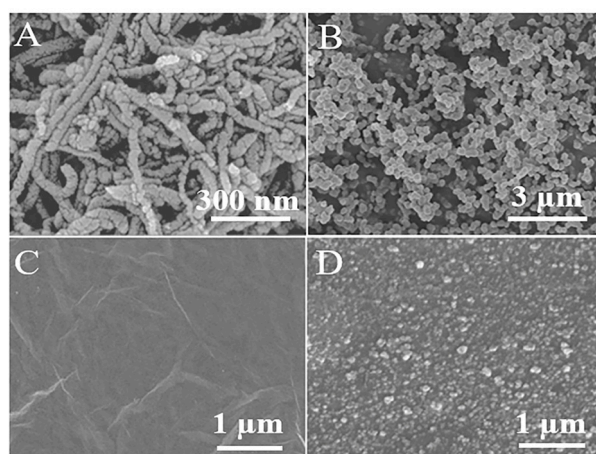


**Figure 1.** SEM of (A)  $\text{Fe}_3\text{O}_4$ @MWNTs; (B)  $\text{MIP@Fe}_3\text{O}_4$ @MWNTs; (C) rGO/MCPE; (D)  $\text{MIP@Fe}_3\text{O}_4$ @MWNTs/rGO/MCPE.

The cyclic voltammogram behaviors of these CPEs, modified with different materials, were measured in 0.1 mol/L KCl solution containing 5.0 mmol/L  $\text{K}_3[\text{Fe}(\text{CN})_6]$  (Figure 2). It was determined that the redox peak of  $\text{K}_3[\text{Fe}(\text{CN})_6]$  on the carbon paste electrode (MCPE) doped with  $\text{Fe}_3\text{O}_4$ @MWNTs (curve b) was significantly larger than that prepared from pure graphite (curve a), indicating that the modification of  $\text{Fe}_3\text{O}_4$ @MWNTs not only brought magnetic properties to the carbon paste electrode, but that it also increased the electron conductivity of the carbon paste electrodes [24]. After the modification of rGO on MCPE, the redox peak of potassium ferricyanide on the electrode further increased, and the peak voltage was shifted in the negative direction (curve c), which proved that the rGO had a substantial enhancement of the conductivity of the carbon paste electrode. After modification of the  $\text{MIP@Fe}_3\text{O}_4$ @MWNTs, the redox peak of potassium ferricyanide (curve d) decreased compared to that before modification (curve c), which was due to the poor conductivity of the molecularly imprinted polymer, indicating that the methacrylate molecularly imprinted polymer was wrapped around the magnetic material  $\text{Fe}_3\text{O}_4$ @MWNTs. When  $\text{MIP@Fe}_3\text{O}_4$ @MWNTs/rGO/MCPE was incubated in the solution containing TMP, the imprinted caves in the imprinted polymer on the electrode surface were partially occupied by TMP, which led to a further decrease in the conductivity of  $\text{MIP@Fe}_3\text{O}_4$ @MWNTs. Thus, the redox peak of potassium cyanide on  $\text{MIP@Fe}_3\text{O}_4$ @MWNTs/rGO/MCPE is also further reduced (curve f). Compared with the imprinted polymer, there were no imprinted caves in the non-imprinted polymer modified  $\text{NIP@Fe}_3\text{O}_4$ @MWNTs/rGO/MCPE electrode, so there are no channels on the electrode surface geometry. The absence of imprinted caves

blocked the diffusion of electroactive substances, resulting in redox peaks of potassium cyanide that were hardly observed on NIP@Fe<sub>3</sub>O<sub>4</sub>@MWNTs/rGO/MCPE (Curve f).

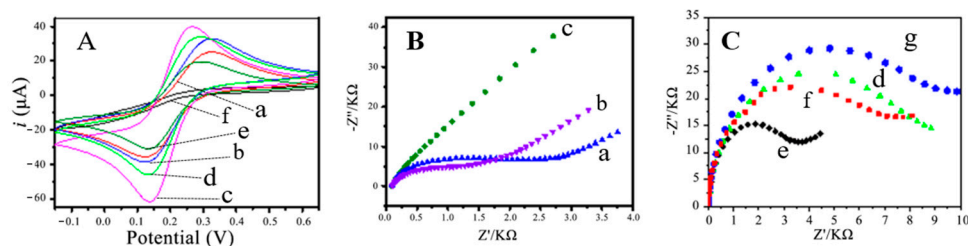


**Figure 2.** (A) Cyclic voltammograms recorded in 0.1 mol/L KCl solution containing 5.0 mmol/L K<sub>3</sub>Fe(CN)<sub>6</sub> for (a) CPE; (b) MCPE; (c) rGO/MCPE; (d) MIP@Fe<sub>3</sub>O<sub>4</sub>@MWNTs/rGO/MCPE; (e) MIP@Fe<sub>3</sub>O<sub>4</sub>@MWNTs/rGO/MCPE after 8 min of incubation in 10.0 μmol/L TMP solution; (f) NIP@Fe<sub>3</sub>O<sub>4</sub>@MWNTs/rGO/MCPE after 8 min incubation in 10.0 μmol/L TMP solution. (B,C) EIS recorded in 5.0 mmol/L K<sub>3</sub>Fe(CN)<sub>6</sub> and 0.1 mol/L KCl for (a) CPE; (b) MCPE; (c) rGO/MCPE; MIP@Fe<sub>3</sub>O<sub>4</sub>@MWNTs/rGO/MCPE before (d) and after (e) elution together with rebinding of TMP (f), and (g) NIP@Fe<sub>3</sub>O<sub>4</sub>@MWNTs/rGO/MCPE.

The results of electrochemical impedance measurement also supported the conclusions obtained by the CV method (Figure 2B,C). According to the order of CPE (Curve a), MCPE (Curve b), and rGO/MCPE (curve c), the impedance decreased in turn, indicating the electrical signal amplification function of Fe<sub>3</sub>O<sub>4</sub>@MWNTs and rGO on carbon paste electrodes. For the electrode modified with the imprinted material, if the template molecules were not washed away from the imprinted material, the impedance was large (Curve d). When the template molecules were washed away, the impedance became substantially smaller (Curve e). In addition, after the imprinted material was combined with the template molecules again, the impedance increased (Curve f), demonstrating that the imprinted sites matching the template molecules formed in the imprinted material. The impedance of NIP@Fe<sub>3</sub>O<sub>4</sub>@MWNTs/rGO/MCPE was the largest (Curve g), further indicating that the non-imprinted polymer did not generate imprinted sites.

### 3.2. Optimization of Preparation Conditions for TMP Molecularly Imprinted Materials

Molecularly imprinted polymers have high adsorption capacity and high recognition selectivity for the target (template molecule), which is a prerequisite to the high sensitivity and high selectivity of molecularly imprinted sensors as recognition elements. For surface-imprinted polymers, when the type of carrier is fixed, the main factors affecting its adsorption capacity and adsorption selectivity include the functional monomer, the cross-linking agent, and the amount of carrier. Thus, as shown in Tables 1 and 2, an orthogonal experiment was carried out to optimize the above four factors. Seventeen imprinted and non-imprinted polymers were prepared according to the experimental conditions in Table 2. The adsorption amounts (Q) of these polymers were determined, and the adsorption selectivity factors (IF) of the imprinted polymers were calculated. The results are shown in Table 2.

**Table 1.** Factor level table of orthogonal test.

Factor Level	Functional Monomer (A)	The Amount of Monomer (mmol) (B)	The Amount of EGDMA (mmol) (C)	The Amount of Fe <sub>3</sub> O <sub>4</sub> @MWNTs (mg) (D)
1	AAA	0.2	3.0	0.05
2	AM	0.3	4.0	0.075
3	MAA	0.4	5.0	0.100
4	NAU	0.5	6.0	0.125

The number of other reactants: The concentration of template molecule (TMP) was 0.1 mmol; the number of initiators (AIBN) was 30 mg, the volume of porous agent acetonitrile was 20 mL, respectively.

**Table 2.** Orthogonal test table.

NO.	Functional Monomer	The Amount of Monomer (mmol)	The Amount of EGDMA (mmol)	The Amount of Fe <sub>3</sub> O <sub>4</sub> @MWNTs (mg)	QMIP	IF
1	(1)	(1)	(2)	(4)	9.7	1.81
2	(1)	(2)	(3)	(2)	13.1	2.17
3	(1)	(3)	(4)	(3)	14.6	2.19
4	(1)	(4)	(1)	(1)	10.2	1.54
5	(2)	(1)	(3)	(1)	6.9	1.36
6	(2)	(2)	(4)	(4)	7.5	1.57
7	(2)	(3)	(1)	(3)	8.1	1.42
8	(2)	(4)	(2)	(2)	6.3	1.28
9	(3)	(1)	(4)	(3)	10.6	1.74
10	(3)	(2)	(1)	(1)	7.3	1.35
11	(3)	(3)	(2)	(2)	9.8	1.62
12	(3)	(4)	(3)	(4)	11.9	1.58
13	(4)	(1)	(1)	(2)	5.1	1.04
14	(4)	(2)	(2)	(4)	6.8	1.51
15	(4)	(3)	(3)	(1)	7.4	1.49
16	(4)	(4)	(4)	(3)	8.7	1.24
17	(1)	(2)	(3)	(3)		

Considering that the main purpose of introducing the imprinted polymer into the sensor was to improve the response selectivity of the sensor, the experiments were conducted with the adsorption selectivity factor of the imprinted polymer as the evaluation parameter. On the basis of this, the results of the experiments in Table 2 were analyzed by a polar difference analysis, and the corresponding results are shown in Table 3.

**Table 3.** The results of range analysis with IF as evaluation index.

Factor Level	Functional Monomer	The Amount of Monomer (mmol)	The Amount of EGDMA (mmol)	The Amount of Fe <sub>3</sub> O <sub>4</sub> @MWNTs (mg)
1	7.71	5.95	5.35	5.74
2	5.63	6.60	6.22	6.11
3	6.29	6.72	6.60	6.59
4	5.28	5.64	6.74	6.47
Range (R)	2.43	1.08	1.39	0.85
Optimal scheme	(1)	(3)	(4)	(3)

As shown in Table 3, for MIP@Fe<sub>3</sub>O<sub>4</sub>@MWNTs, the important factor affecting the adsorption selectivity factor was the functional monomer among the four factors. AAA was the most suitable among the four monomers, followed by MAA, probably because both AAA and MAA possessed carboxyl groups and were acidic molecules, while TMP contained amino group and nitrogen atoms, which belonged to alkaloids. Thus, AAA and MAA can bind to TMP by hydrogen bonds between carboxyl groups and amino groups. The amount of functional monomers, as well as EGDMA, also had a significant effect on the adsorption selectivity factor of MIP@Fe<sub>3</sub>O<sub>4</sub>@MWNTs, which showed a trend of increasing and then decreasing for the adsorption selectivity factor with the increase of the amount. As shown in Table 3, in terms of the adsorption selectivity factor, the optimal experimental scheme was A1B3C4D3, i.e., the Group 3 experiments in Table 2, and the adsorption selectivity factor of MIP@Fe<sub>3</sub>O<sub>4</sub>@MWNTs prepared under this experimental condition was 2.19, and the adsorption amount also reached 14.6 mg/g. Therefore, the optimal preparation conditions of MIP@Fe<sub>3</sub>O<sub>4</sub>@MWNTs were shown as follows: AAA was used as the functional monomer, and the amounts of AAA, EGDMA, and Fe<sub>3</sub>O<sub>4</sub>@MWNTs were 51.6 mg, 1189.3 mg, and 0.100 mg, respectively.

### 3.3. The Detection of TPM Using MIP@Fe<sub>3</sub>O<sub>4</sub>@MWNTs/rGO/MCPE

Since TMP can be oxidized near 1.1 V on MIP@Fe<sub>3</sub>O<sub>4</sub>@MWNTs/rGO/MCPE, the determination of TMP was conducted by the direct DPV method, and the electrolyte solution and incubation time were optimized in the following part. Considering that TMP has better solubility in acidic media, the DPV peak current values of MIP@Fe<sub>3</sub>O<sub>4</sub>@MWNTs/rGO/MCPE for TMP with a concentration of  $1.0 \times 10^{-5}$  mol/L in 0.1 mol/L sulfuric acid, acetic acid, and phosphoric acid media (all containing 0.1 mol/L KCl) were measured. The results showed that the DPV peak current exhibited a maximum value in H<sub>2</sub>SO<sub>4</sub> solution (Figure 3A). The concentration of H<sub>2</sub>SO<sub>4</sub> solution was further optimized in the range of ~0.01–0.15 mol/L. As depicted in Figure 3B, the best result could be obtained when the concentration of sulfuric acid was 0.1 mol/L. Therefore, 0.1 mol/L H<sub>2</sub>SO<sub>4</sub> containing 0.1 mol/L KCl was chosen as the electrolyte solution for the following experiment.

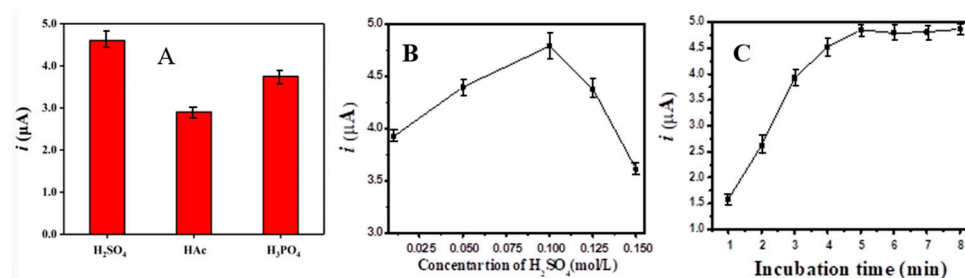


**Figure 3.** Effect of (A) the types of supporting electrolyte solutions and (B) the concentration of H<sub>2</sub>SO<sub>4</sub> on the peak current response to  $1.0 \times 10^{-5}$  mol/L TMP. (C) Effect of incubation time on the peak current response to  $1.0 \times 10^{-5}$  mol/L TMP.

The effect of incubation time on the DPV peak current was investigated at a voltage of  $-0.2$  V. As displayed in Figure 3C, the peak current of  $1.0 \times 10^{-5}$  mol/L TMP in MIP@Fe<sub>3</sub>O<sub>4</sub>@MWNTs/rGO/MCPE gradually increased with the increasing incubation time and displayed a maximum value when the incubation time reached 5 min. Therefore, the incubation time selected for the experiment was 5 min.

Figure 4A shows the DPV response curves of MIP@Fe<sub>3</sub>O<sub>4</sub>@MWNTs/rGO/MCPE to different concentrations of TMP in 0.1 mol/L H<sub>2</sub>SO<sub>4</sub> solution containing 0.1 mol/L KCl. It can be observed that the DPV peak currents increase with an increase in TMP concentration. As shown in Figure 4A, the logarithm of DPV peak current ( $i_p$ ,  $\mu\text{A}$ ) was plotted against the logarithm of TMP concentration ( $c$ , in mol/L). There were two different linear relationships between the logarithm of DPV peak current and the logarithm of TMP concentration in the range of  $4.0 \times 10^{-9}$ – $8.0 \times 10^{-8}$  mol/L and  $8.0 \times 10^{-8}$ – $5.0 \times 10^{-4}$  mol/L (Figure 4B). The corresponding linear regression equations were  $\lg i_p = -5.441 + 0.0418 \lg c$  ( $r^2 = 0.9878$ ) and  $\lg i_p = -3.922 + 0.279 \lg c$  ( $r^2 = 0.9950$ ), respectively. Based on  $S/N = 3$ , the limit of detection of the method was calculated to be  $1.2 \times 10^{-9}$  mol/L. The new method based on this electrochemical sensor was deemed suitable for the regulatory monitoring of these drugs. To check the selectivity of the sensor, the DPV behaviors of other compounds with a structure similar to TMP, including SMZ, SDZ, CAX, GLU, and urea on MIP@Fe<sub>3</sub>O<sub>4</sub>@MWNTs/rGO/MCPE, were investigated. As shown in Figure 4C, the sensor displayed good selectivity toward TMP. The high sensitivity and selectivity of our electrochemical sensor can be benefited by the synergy effect between molecularly imprinted materials and electrochemical signal amplification materials. As is well-known, molecularly imprinted materials possess high adsorption capacities and excellent recognition selectivity towards targets, which have been introduced as selective recognition elements to upgrade the performance of chemical sensors. Moreover, MWNTs and rGO with good conductivity served as dual signal-amplification materials, which can further improve the response sensitivity of the sensor.

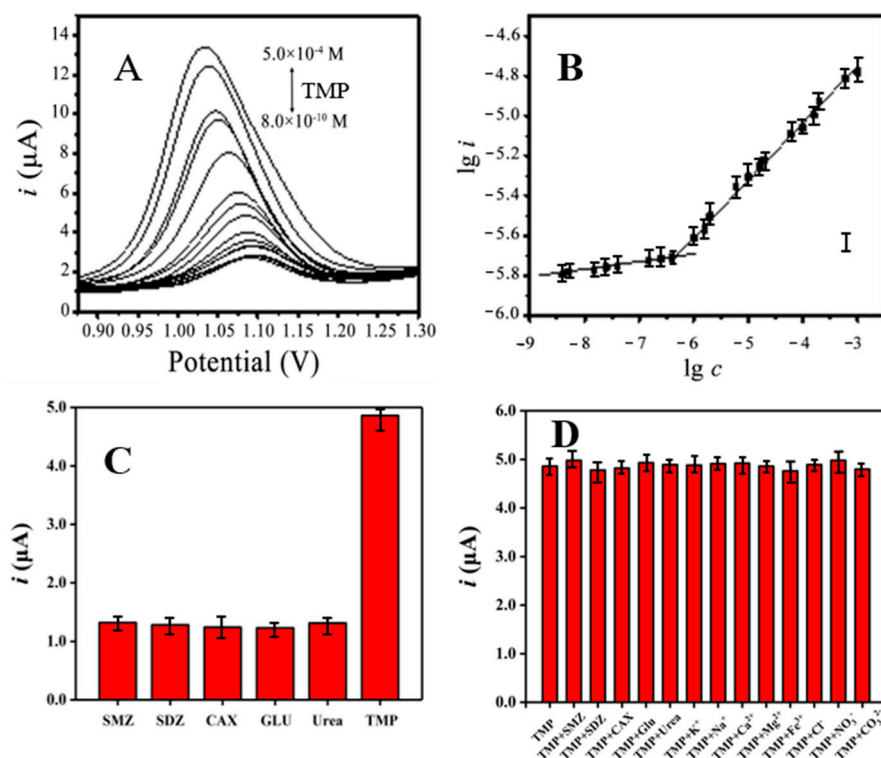


**Figure 4.** (A) Differential pulse voltammetry of MIP@Fe<sub>3</sub>O<sub>4</sub>@MWNTs/rGO/MCPE in the different concentration of TMP; (B) the relationship between the logarithm of peak current ( $i$ ) and the logarithm of TMP concentration; (C) the peak current of MIP@Fe<sub>3</sub>O<sub>4</sub>@MWNTs/rGO/MCPE for  $1.0 \times 10^{-5}$  mol/L SMZ, SDZ, CAX, GLU, urea, and TMP, respectively. The concentration of SMZ, SDZ, CAX, GLU, urea, and TMP was  $1.0 \times 10^{-5}$  mol/L. (D) Effects of different interfering substances on the peak current of MIP@Fe<sub>3</sub>O<sub>4</sub>@MWNTs/rGO/MCPE for  $1.0 \times 10^{-5}$  mol/L TMP. The concentration of SMZ, SDZ, and CAX was  $1.0 \times 10^{-4}$  mol/L, and the concentration for Glu, urea, K<sup>+</sup>, Na<sup>+</sup>, Ca<sup>2+</sup>, Mg<sup>2+</sup>, Fe<sup>3+</sup>, Cl<sup>-</sup>, NO<sub>3</sub><sup>-</sup>, and CO<sub>3</sub><sup>2-</sup> was  $1.0 \times 10^{-3}$  mol/L.

In order to investigate the anti-interference ability of MIP@Fe<sub>3</sub>O<sub>4</sub>@MWNTs/rGO/MCPE to detect TMP, the electrochemical behaviors were performed by adding  $1.0 \times 10^{-4}$  mol/L of SMZ, SDZ, and CAX, as well as  $1.0 \times 10^{-3}$  mol/L of Glu, urea, K<sup>+</sup>, Na<sup>+</sup>, Ca<sup>2+</sup>, Mg<sup>2+</sup>, Fe<sup>3+</sup>, Cl<sup>-</sup>, NO<sub>3</sub><sup>-</sup>, and CO<sub>3</sub><sup>2-</sup> to  $1.0 \times 10^{-5}$  mol/L of TMP solution, respectively. A series of mixed solutions of TMP and other components were prepared. As shown in Figure 4D, the DPV peak currents of MIP@Fe<sub>3</sub>O<sub>4</sub>@MWNTs/rGO/MCPE in these mixed solutions were measured. It could be observed that SMZ, SDZ, CAX, glucose, and urea did not interfere with the determination of TMP when the allowable error was less than or equal to 5%, demonstrating that the sensor possessed good anti-interference ability and had good application prospects for practical sample analysis.

To further investigate the stability and repeatability of the prepared MIP@Fe<sub>3</sub>O<sub>4</sub>@MWNTs/rGO/MCPE, five electrodes were prepared in the same way and used to detect TMP with a concentration of  $1.0 \times 10^{-5}$  mol/L under the same conditions. The results showed that the RSD value of the DPV peak current obtained by these five electrodes was 6.2%. When the electrode was used 60 times, the DPV current of TMP with the same concentration reached 92.3% of its initial value. In addition, when the electrode was stored in water and kept in a refrigerator (4 °C) for 2 months, the DPV current of TMP with the same concentration still reached 91.7% of its initial value. The above results showed the excellent stability and reproducibility of MIP@Fe<sub>3</sub>O<sub>4</sub>@MWNTs/rGO/MCPE prepared by this method, which revealed that the electrochemical sensor had practical value.

### 3.4. Real Sample Analysis

Considering TMP is a broad-spectrum antimicrobial agent, it is very important to determine the concentration in a urine sample to investigate its measured result [25]. The treated samples (environmental water samples, human urine samples, and cefadroxil capsules, 1.0 mL) were added to 9 mL of 0.1 mol/L H<sub>2</sub>SO<sub>4</sub> solution containing 0.1 mol/L KCl and mixed well for the determination by MIP@Fe<sub>3</sub>O<sub>4</sub>@MWNTs/rGO/MCPE. In order to verify the accuracy of the results, spiked recovery experiments were also performed for different samples, as shown in Table 4. According to the results for the determination of trimethoprim in real samples (n = 5), TMP was not detected in the environmental water samples or human urine samples, and the measured value of TMP in the solution of cefadroxil meperidine capsules was 16.90 μmol/L, which was equivalent to 12.27 mg of meperidine per capsule and essentially consistent with the labeled amount (12.50 mg). The recoveries of all spiked samples were determined to be between 91% and 110%, and RSD values were within 6%. It demonstrated that the prepared MIP@Fe<sub>3</sub>O<sub>4</sub>@MWNTs/rGO/MCPE was accurate and reliable for the detection of meperidine in environmental water samples, human urine samples, and meperidine drugs with practicality.

**Table 4.** Results for the determination of trimethoprim in real samples (n = 5).

Sample	Added (μmol/L)	Found (μmol/L)	Recovery (%)	RSD (%)
Kunming Panlong river water	0	ND *	-	-
	0.010	0.0091	91.0	4.97
	1.00	0.94	94.0	3.85
	50.0	49.6	99.2	3.14
Healthy human urine	0	ND *	-	-
	0.010	0.011	110.0	5.73
	1.00	0.95	95.0	4.36
	50.0	51.6	103.2	3.14
Cefadroxil capsules	0	16.90	-	2.16
	5.0	21.84	98.8	2.01
	15	32.60	104.7	1.98
	30	47.74	102.8	3.37

\* 'ND' means none.

## 4. Conclusions

In order to obtain stable and highly sensitive TMP molecularly imprinted electrochemical sensors, MIP@Fe<sub>3</sub>O<sub>4</sub>@MWNTs/rGO/MCPE was fabricated by involving multiple functional materials. MWNTs-doped Fe<sub>3</sub>O<sub>4</sub> magnetic composites were prepared as modification materials for carbon paste electrodes and carriers for the preparation of molecularly imprinted materials, which not only increased the electrical conductivity and electrocatalytic activity of carbon paste electrodes as well as molecularly imprinted materials, but also improved the binding force between the base electrode and the imprinting material. Meanwhile, chitosan was introduced as a binder between the molecular imprinting material and the electrode surface to further ensure the bonding firmness of the molecular-imprinting material on the electrode surface. Furthermore, a layer of rGO was modified on the surface of the magnetic carbon paste electrode as a signal amplifier element to further ensure the response sensitivity of the electrode. The results showed that the imprinted sensor constructed in this paper was stable, sensitive, and resistant to interference, and the detection limit reached  $1.2 \times 10^{-9}$  mol/L. Compared with previous electrochemical methods, including those based on molecular imprinted sensors (see Table 5 for a comparison of electrochemical analysis methods for the determination of trimethoprim) for the determination of TMP reported in the literature, the sensor had a high sensitivity and wide linear range for the detection of TMP, which can be attributed to the integration and synergy effect of these functional materials.

**Table 5.** Comparison of electrochemical analysis methods for determination of trimethoprim.

Electrode	Test Method	Linear Range ( $\mu\text{mol/L}$ )	Detection Limit ( $\mu\text{mol/L}$ )	Reference
GCE	DPV	20.0~4200	4.0	[11]
EGCE	DPV	12.5~30.0	0.082	[12]
HMDE	AdCSV	0.1~1.0	0.01	[13]
MWCNT/PBnc/SPE	DPV	10.0~100.0	0.06	[14]
GR-ZnO/GCE	DPV	1.0~180.0	0.30	[15]
CuPh/PC/GCE	DPV	0.4~1.1	0.60	[16]
		1.5~6.0		
rGNRs/SPCEs	DPV	1.0~10.0	0.04	[17]
rGO-AgNP/GCE	DPV	1.0~10.0	0.40	[18]
MWCNTs-Nafion/GCE	LSV	5.0~1000.0	0.66	[19]
SP-MWCNT-SbNP/CPE	DPV	0.1~0.7	0.031	[20]
SBA/Ti-3/MWCNT/CPE	DPV	0.2~20.0	0.07	[21]
MIP/G/GCE	SWV	1.0~100.0	0.13	[22]
MIP/Nano-Pd/GCE	DPV	0.5~4000.0	0.032	[23]
		0.004~0.08		
MIP@Fe <sub>3</sub> O <sub>4</sub> @MWNTs/rGO/MCPE	DPV	0.08~500.0	0.0012	This work

**Author Contributions:** P.L.: formal analysis, data curation, and writing original draft; R.Z.: investigation, methodology, and writing review& editing; L.Z. and Q.C.: resources, funding acquisition, and writing review and editing. All authors have read and agreed to the published version of the manuscript.

**Funding:** This research was funded by the National Natural Science Foundation of China grant number [21964020, 21962022, 22164020] and Open project of the Key Laboratory of Drug Analysis and Anti-Drug Technology of the Ministry of Public Security [2019DPKF01].

**Institutional Review Board Statement:** Not applicable.

**Informed Consent Statement:** Not applicable.

**Data Availability Statement:** Do not have the supporting reported results.

**Acknowledgments:** This research was funded by the National Natural Science Foundation of China grant number [22164020] and Open project of the Key Laboratory of Drug Analysis and Anti-Drug Technology of the Ministry of Public Security [2019DPKF01].

**Conflicts of Interest:** The authors declare no conflict of interest.

## Abbreviations

TMP	Trimethoprim
MWNTs	Multi-walled carbon nanotubes
MCPE	Magnetic molecularly imprinted carbon paste electrode
rGO	Reduction graphene oxide
RSD	Relative standard deviation
MIP@Fe <sub>3</sub> O <sub>4</sub> @MWNTs/rGO/MCPE	TMP molecularly imprinted electrochemical sensor
CV	Cyclic voltammetry
DPV	Differential pulse voltammetry
EIS	Electrochemical impedance spectroscopy
TMP	Trimethoprim
SMZ	Sulfamethoxazole
SDZ	Sulfadiazin
CAX	Cephalexin
Glu	Glucose
MAA	Methylalanic acid
AAA	2-acetamide acrylic acid
AM	Acrylamide
NAU	N-Allyl urea
EGDMA	Glycol dimethacrylate
AIBN	Azodiisobutyronitrile

## References

1. Berendsen, B.J.A.; Roelofs, G.; van Zanten, B.; Driessen-van Lankveld, W.D.M.; Pikkemaat, M.G.; Bongers, I.E.A.; de Lange, E. A strategy to determine the fate of active chemical compounds in soil; applied to antimicrobially active substances. *Chemosphere* **2021**, *279*, 130495. [[CrossRef](#)] [[PubMed](#)]
2. Arbab, S.; Ullah, H.; Wang, W.; Zhang, J. Antimicrobial drug resistance against *Escherichia coli* and its harmful effect on animal health. *Veter Med. Sci.* **2022**, *8*, 1780–1786. [[CrossRef](#)] [[PubMed](#)]
3. Walzer, P.D.; Foy, J.; Steele, P.; White, M. Treatment of experimental pneumocystosis: Review of 7 years of experience and development of a new system for classifying antimicrobial drugs. *Antimicrob. Agents Chemother.* **1992**, *36*, 1943–1950. [[CrossRef](#)] [[PubMed](#)]
4. Yang, Y.J.; Liu, X.W.; Li, B.; Li, S.H.; Kong, X.J.; Qin, Z.; Li, J.Y. Simultaneous determination of diaveridine, trimethoprim and ormetoprim in feed using high performance liquid chromatography tandem mass spectrometry. *Food Chem.* **2016**, *212*, 358–366. [[CrossRef](#)] [[PubMed](#)]
5. Horvath, Z.; Sali, J.; Zentai, A.; Doroghazi, E.; Farkas, Z.; Kerekes, K.; Ambrus, A. Limitations in the determination of maximum residue limits and highest residues of pesticides: Part I. *J. Environ. Sci. Health B* **2014**, *49*, 143–152. [[CrossRef](#)]
6. Hruska, M.W.; Frye, R.F. Determination of trimethoprim in low-volume human plasma by liquid chromatography. *J. Chromatogr. B Anal. Technol. Biomed. Life Sci.* **2004**, *807*, 301–305. [[CrossRef](#)]
7. Rehm, S.; Rentsch, K.M. LC-MS/MS method for nine different antibiotics. *Clin. Chim. Acta* **2020**, *511*, 360–367. [[CrossRef](#)]
8. Choi, S.Y.; Kang, H.-S. Multi-Residue Determination of Sulfonamides, Dapsone, Ormethoprim, and Trimethoprim in Fish and Shrimp Using Dispersive Solid Phase Extraction with LC-MS/MS. *Food Anal. Methods* **2021**, *14*, 1256–1268. [[CrossRef](#)]
9. Soudi, A.T.; Hussein, O.G.; Elzanfaly, E.S.; Zaazaa, H.E.; Abdelkawy, M. Simultaneous determination of phenazopyridine HCl and trimethoprim in presence of phenazopyridine HCl impurity by univariate and multivariate spectrophotometric methods—Quantification of phenazopyridine HCl impurity by univariate methods. *Spectrochim. Acta A Mol. Biomol. Spectrosc.* **2020**, *239*, 118516. [[CrossRef](#)]
10. Liu, L.; Wan, Q.; Xu, X.; Duan, S.; Yang, C. Combination of micelle collapse and field-amplified sample stacking in capillary electrophoresis for determination of trimethoprim and sulfamethoxazole in animal-originated foodstuffs. *Food Chem.* **2017**, *219*, 7–12. [[CrossRef](#)]
11. Guaraldo, T.T.; Goulart, L.A.; Moraes, F.C.; Lanza, M.R.V. Carbon black nanospheres modified with Cu (II)-phthalocyanine for electrochemical determination of Trimethoprim antibiotic. *Appl. Surf. Sci.* **2019**, *470*, 555–564. [[CrossRef](#)]
12. Zhang, W.; Zhang, C.; Jiao, Z.; Zhu, H.; Xu, G.; Chen, X.; Liu, B.; Tang, Y. Electrochemical behavior of matrix graphite in nitric acid by cyclic voltammetry. *J. Nucl. Mater.* **2023**, *581*, 154411. [[CrossRef](#)]
13. Sgobbi, L.F.; Razzino, C.A.; Machado, S.A.S. A disposable electrochemical sensor for simultaneous detection of sulfamethoxazole and trimethoprim antibiotics in urine based on multiwalled nanotubes decorated with Prussian blue nanocubes modified screen-printed electrode. *Electrochim. Acta* **2016**, *191*, 1010–1017. [[CrossRef](#)]
14. Carapuca, H.M.; Cabral, D.J.; Rocha, L.S. Adsorptive stripping voltammetry of trimethoprim: Mechanistic studies and application to the fast determination in pharmaceutical suspensions. *J. Pharm. Biomed. Anal.* **2005**, *38*, 364–369. [[CrossRef](#)]
15. Yue, X.; Li, Z.; Zhao, S. A new electrochemical sensor for simultaneous detection of sulfamethoxazole and trimethoprim antibiotics based on graphene and ZnO nanorods modified glassy carbon electrode. *Microchem. J.* **2020**, *159*, 105440. [[CrossRef](#)]
16. Martins, T.S.; Bott-Neto, J.L.; Oliveira Jr, O.N.; Machado, S.A.S. Paper-based electrochemical sensors with reduced graphene nanoribbons for simultaneous detection of sulfamethoxazole and trimethoprim in water samples. *J. Electroanal. Chem.* **2021**, *882*, 114985. [[CrossRef](#)]
17. Golinelli, D.L.C.; Machado, S.A.S.; Cesarino, I. Synthesis of Silver Nanoparticle-Graphene Composites for Electroanalysis Applications using Chemical and Electrochemical Methods. *Electroanalysis* **2017**, *29*, 1014–1021. [[CrossRef](#)]
18. D'Souza, O.J.; Mascarenhas, R.J.; Satpati, A.K.; Detriche, S.; Mekhalif, Z.; Delhalle, J.; Dhasan, A. High electrocatalytic oxidation of folic acid at carbon paste electrode bulk modified with iron nanoparticle-decorated multiwalled carbon nanotubes and its application in food and pharmaceutical analysis. *Ionics* **2016**, *23*, 201–212. [[CrossRef](#)]
19. Cesarino, I.; Cesarino, V.; Lanza, M.R.V. Carbon nanotubes modified with antimony nanoparticles in a paraffin composite electrode: Simultaneous determination of sulfamethoxazole and trimethoprim. *Sens. Actuators B Chem.* **2013**, *188*, 1293–1299. [[CrossRef](#)]
20. De Souza, L.V.; Tkachenko, O.; Cardoso, B.N.; Pizzolato, T.M.; Dias, S.L.P.; Vasconcellos, M.A.Z.; Arenas, L.T.; Costa, T.M.H.; Moro, C.C.; Benvenuti, E.V. Strategy to control the amount of titania dispersed on SBA-15 surface preserving its porosity, aiming to develop a sensor for electrochemical evaluation of antibiotics. *Microporous Mesoporous Mater.* **2019**, *287*, 203–210. [[CrossRef](#)]
21. Da Silva, H.; Pacheco, J.G.; Magalhaes, J.M.; Viswanathan, S.; Delerue-Matos, C. MIP-graphene-modified glassy carbon electrode for the determination of trimethoprim. *Biosens. Bioelectron.* **2014**, *52*, 56–61. [[CrossRef](#)] [[PubMed](#)]
22. Fan, P.; Wang, B. Preparation of molecularly imprinted polymer membrane with blending trimethoprim-MIP and polysulfone and its transport properties. *Korean J. Chem. Eng.* **2010**, *26*, 1813–1820. [[CrossRef](#)]
23. Zhang, Q.; Zhu, M.; Zhang, Q.; Li, Y.; Wang, H. The formation of magnetite nanoparticles on the sidewalls of multi-walled carbon nanotubes. *Compos. Sci. Technol.* **2009**, *69*, 633–638. [[CrossRef](#)]

24. Madrakian, T.; Asl, K.D.; Ahmadi, M.; Afkhami, A. Fe<sub>3</sub>O<sub>4</sub>@Pt/MWCNT/carbon paste electrode for determination of a doxorubicin anticancer drug in a human urine sample. *RSC Adv.* **2016**, *6*, 72803–72809. [[CrossRef](#)]
25. Jürg Oliver Straub. An Environmental Risk Assessment for Human-Use Trimethoprim in European Surface Waters. *Antibiotics* **2013**, *2*, 115–162. [[CrossRef](#)]

**Disclaimer/Publisher's Note:** The statements, opinions and data contained in all publications are solely those of the individual author(s) and contributor(s) and not of MDPI and/or the editor(s). MDPI and/or the editor(s) disclaim responsibility for any injury to people or property resulting from any ideas, methods, instructions or products referred to in the content.